FULafia Journal of Science & Technology
ISSN (print) 2449-0954 \ ISSN (online) 2636-4972
https://lafiascijournals.org.ng/index.php/fjst
Sponsored By TERTIARY EDUCATION TRUST FUND
Manuscript => Received: Jan., 2024; Accepted: April, 2024; Published: May, 2024
https://doi.org/10.62050/fjst2024.v8n1.279

CUCURBITA PEPO FLOWER EXTRACT AS A CORROSION INHIBITOR FOR MILD STEEL IN ACIDIC MEDIUM

E. E. Elachi[1]* and E. U. Godwin-Nwakwasi[2]
[1]*Department of Mechanical Engineering, Taraba State University, Jalingo, Taraba State*
[2]*Department of Chemistry, Gregory University, Uturu, Abia State*
*Corresponding email: eeengineer79@gmail.com

ABSTRACT
An investigation into the corrosion inhibition potentials of *Cucurbita pepo* flower was undertaken. The gravimetric and gasometric methods of corrosion measurement were employed at temperatures of 30 and 60°C. Ethanoic extract of *Cucurbita pepo* flower was used as a corrosion inhibitor in 0.5 M HCl solution. The results revealed that it mitigated the corrosion of mild steel in the acidic medium. The inhibition efficiency of the plant increased with concentration and it was found to be temperature dependent. The experimental data fitted to the Temkin adsorption isotherm model. A mechanism of physical adsorption is proposed for the corrosion inhibition process. This work shows the possibility of using *Cucurbita pepo* flower as a corrosion inhibitor.

Keywords: Acidic medium; corrosion inhibition; *Cucurbita pepo*; inhibition efficiency; physical adsorption

INTRODUCTION

One the commonest methods of protecting metals and their alloys from corrosives is by the use of corrosion inhibitors which are low cost, easy to apply and high efficiency (Umoren and Eduok, 2016; Ogunleye *et al*., 2020). Synthetic corrosion inhibitors have successfully been used to control the corrosion of metals in various media (Loto *et al*., 2017; Lgaz *et al*. 2020). The use of synthetic inhibitors is being restricted due to their adverse effects on man, animals and the environment (Bucaretchi *et al*., 2003). Plants are used as substitutes for synthetic inhibitors because they are cheap, readily available and environmentally friendly (Al-Otaibi *et al*., 2012; Hassan *et al*., 2016). Several plants have successfully been used to control the corrosion of metals in various media. One of such plants is *Cucurbita pepo* (Pumpkin). According to Chahul *et al*. (2019), the ethanol extract of the leaves of *Cucurbita pepo* inhibited the corrosion of mild steel in acidic medium. However, perusal of literature showed that the flower of *Cucurbita pepo* has not been investigated for its corrosion inhibition potentials.

Therefore, the objective of this paper is to investigate the inhibitive effects of the flower extract of *Cucurbita pepo* in hydrochloric acid medium.

MATERIALS AND METHOD

Pretreatment of plant materials

The pretreatment of *Cucurbita pepo* flower was carried out using method previously described by Elachi *et al*. (2022).

Soxhlet extraction

Soxhlet extractor was used to extract the active ingredients in the powdered plant material. Three hundred (300 mL) of absolute ethanol was poured into a boiling flask. Seventy grammes of the powdered plant material was placed in the thimble and inserted in the extraction chamber. Fitted with a reflux condenser, the set-up was heated at a temperature of 78°C. Extraction was allowed to continue until the solvent in the siphon becomes clear (colourless). This is an indication that extraction is completed (Hussain, 2023). The ethanol was recovered using a rotary evaporator and the crude product was obtained. The required concentrations (0.2 g/L, 0.4 g/L, 0.6 g/L, 0.8 g/L and 1.0 g/L) were prepared from the extract using 0.5 M HCl solution.

Fourier transform infrared spectroscopy (FTIR) analysis

FTIR analysis of the pure extract and the corrosion environment (0.5 M HCl solution with 1.0 g/L of the extract) after test were carried out to determine the compounds present (Iorhuna and Ayuba, 2023). The extract and corrosion environment were each scanned at a wavelength of 500-4000 cm^{-1} to obtain their respective IR spectra using Buckscientific FTIR spectrophotometer (Model: M530).

Preparation of corrosion test specimens

Corrosion coupons (4.00 cm×2.50 cm×1.92 cm) were prepared from mild steel sheet using methods described previously by Obot *et al*. (2011) and Giwa *et al*. (2020).

Gravimetric method

Gravimetric measurements were conducted in duplicates at temperatures of 30 and 60°C using methods previously described by Ibisi and Ugochukwu (2015); Chahul *et al*. (2019) and Giwa *et al*. (2020). Pre-weighed test specimens were immersed in beakers each containing 0.5 M HCl solution and various concentrations (0.0, 0.2, 0.4, 0.6, 0.8 and 1.0 g/L) of the extract for ten hours. Test specimens were retrieved after every two hours, scrubbed with a nylon brush under running water, cleaned with ethanol and dried in acetone. The corrosion rates were computed from the weight loss data using Equation 1 (Uwah *et al*., 2013).

$$CR = \frac{W}{At} \qquad 1$$

where CR is the corrosion rate in $gcm^{-2}hr^{-1}$, w is the weight loss in grammes, A is the specimen surface area in cm^2 and t is the exposure time in hours.

The inhibition efficiency was computed using the expression in Equation 2 (Chahul *et al*., 2019).

$$IE = (1 - \frac{w_1}{w_2}) \times 100 \qquad 2$$

where IE is inhibition efficiency, w_1 is weight loss in the presence of the inhibitor in grammes and w_2 is weight loss in the absence of the inhibitor in grammes

Gasometric method

Hydrogen evolution measurements were performed using the gasometric technique previously described by Obot *et al*. (2011); Abdulrahman *et al*. (2015). The rate of hydrogen evolution (CR_H) was determined from the slope of the graph of the volume of gas evolved (V) versus time (t) using Equation 3 (Obot *et al*., 2011).

$$CR_H = \frac{V_t - V_i}{t_t - t_i} \qquad 3$$

where V_t and V_i are the volumes of hydrogen evolved at time t_t and t_i respectively.

The inhibition efficiency of the extract was calculated using the expression in Equation 4 (Obot *et al*., 2011)

$$IE = \frac{CR_{blank} - CR_{inh}}{CR_{blank}} \times 100 \qquad 4$$

Where CR_{blank} $and CR_{inh}$ are the hydrogen evolution rates in the absence and presence of the extract.

RESULTS AND DISCUSSION

Interpretation of FTIR analysis of the pure extract

The functional groups and the possible compounds from the FTIR analysis of the pure extract is presented in Table 1. The result revealed the presence of compounds such as aromatics, aliphatics, amines, aldehydes, carboxylic acids, alcohols etc in the extract. These compounds contain heteroatoms like nitrogen, sulphur and oxygen in their structures which have the ability to adsorb onto the metal surface (Fadare *et al*., 2016). Therefore, the flower extract of *Cucurbita pepo* has corrosion inhibition potentials. Similar results were reported by Giwa *et al*. (2020); Erebugha *et al*. (2021); Iorhuna and Ayuba (2023).

Table 1: FTIR analysis result of the pure extract (Nandiyanto *et al*., 2019; Stuart, 2004)

Wavelength (Cm^{-1})	Possible functional group
733.0289	C-H stretch, Aromatics
853.4469	C-H stretch, Aromatics
1055.572	C-N stretch, Aliphatic amines
1409.255	C-C stretch, aromatics
1633.158	N-H stretch, 1^0 Amines bend
1971.421	C=C=C stretch, Allen
2046.832	N=C=S stretch, Isothiocyanate
2195.806	C=C stretch, Alkenes
2458.992	C-H stretch, Aldehydes
2671.274	O-H stretch, carboxylic acid
2874.989	C-H stretch, Alkanes
2999.364	O-H stretch, Alcohol
3203.6	O-H stretch, carboxylic acid
3287.603	N-H stretch, aliphatic primary amines
3476.899	N-H stretch, Primary amine

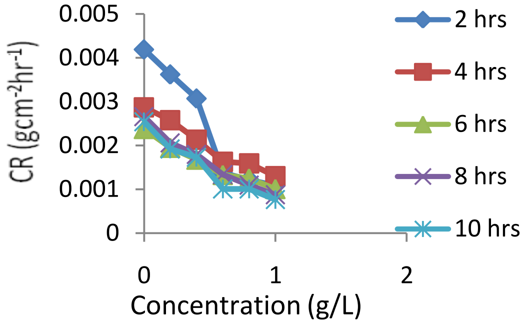

Figure 1: Effect of extract concentration on corrosion rate at 30°C in acidic medium

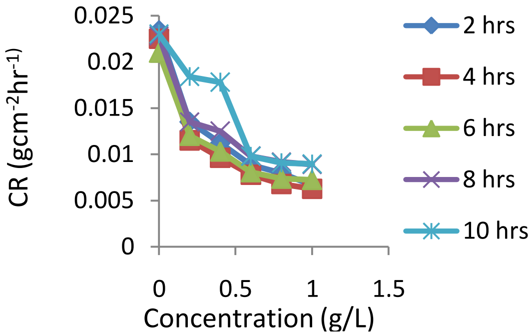

Figure 2: Effect of extract concentration on corrosion rate at 60°C in the acidic medium

Effect of extract (*Cucurbita pepo* flower) concentration on corrosion rate

Figures 1 and 2 show the effect of extract (*Cucurbita pepo* flower) concentration on the corrosion rate of mild steel obtained by gravimetric method.

Corrosion rates were observed to be higher in the blank (0.0 g/L) solution compared to solutions with various concentrations (0.2, 0.4, 0.6, 0.8 and 1.0 g/L) of the extract. This is an indication that the *Cucurbita pepo* extract inhibited the corrosion of the metal in the acidic medium (Iorhuna and Ayuba, 2023). Similar trend was also observed by Chahul *et al*. (2019). A comparison of the results of the FTIR analysis of the pure extract (Table 1) and the acid solutions after test (Tables 2 and 3) at 30 and 60°C revealed that there is an alkane (C-H) shift from 2874.989 to 2891.54 cm^{-1}; aromatic (C-C) shift from 1409.255 to 1423.8 cm^{-1}; aldehyde (C-H) shift from 2458.992 to 2705.333 cm^{-1}; amine (N-H) shift from 1633.158 to 1622.682 cm^{-1}; isothiocyanate (N=C=S) shift from 2046.832 to 2059.512 cm^{-1}; and alkyne (C≡C) shift from 2195.806 to 3304.407 cm^{-1} at 30°C. Also at 60°C, there is an alkane (C=C=C) shift from 1971.421 to 1996.498 cm^{-1}; aldehyde (C-H) shift from 2458.992 to 2462.109 cm^{-1}; carboxylic acid (O-H) shift from 3203.6 to 3226.25 cm^{-1}; alkane (C-H) shift from 2874.989 to 2851.588 cm^{-1}; alcohol (O-H) shift from 2999.364 to 3011.492 cm^{-1}; aliphatic primary amine (N-H) shift from 3287.603 to 3357.995 cm^{-1}; and primary amine (N-H) shift from 3476.899 to 3438.906 cm^{-1}. The shift in adsorption bands signifies interaction between the metal and the various functional groups present in the extract (Ayuba and Abubakar, 2021). The interaction reduced the surface area available for corrosion reactions. Consequently, the rate of corrosion is lower in solution (s) containing the extract compared to solution without the extract. Corrosion rates were also observed to decrease with increase in the concentration of the extract. Similar result was also obtained by Chahul *et al.* (2019).

Table 2: FTIR analysis result of the acid solution after test at 30°C

Wavelength (cm^{-1})	Possible functional groups
719.6555	C-H stretch, Alkanes
1061.034	C-O stretch, Alkyl aryl ether
1286.124	C-H (-CH_2X), Alkyl halides
1423.8	C-C stretch, Aromatics
1622.682	N-H, 1^0 amines bend
2059.512	N=C=S stretch, Isothiocyanate
2705.333	C-H stretch, Aldehyde
2891.541	C-H stretch, Alkane
3304.407	-C≡C-H, stretch Akynes

Table 3: FTIR analysis result of the acid solution after test at 60°C

Wavelength (cm^{-1})	Possible functional group
765.5796	C-Cl stretch, Alkyl halides
833.4854	C-Cl stretch, Alkyl halides
1001.849	C-O stretch, Alcohols, Carboxylic acids, Esters, Ethers
1206.019	C-H (-CH_2X), Alkyl halides
1275.542	C-N stretch, aromatic amines
1397.308	C-F stretch, Fluoro compound
1621.139	C=C stretch, Conjugated Alkene
1852.541	C-H stretch, aromatic compound bend
1996.498	C=C=C, stretch Allene
2173.363	S-C≡N stretch, thiocyanate
2462	C-H stretch, aldehyde
2560.288	S-H stretch, Thiol
2710.621	O-H stretch, Alcohol
2851.588	C-H stretch, Alkane
3011.492	O-H stretch, Alcohol
3226.25	O-H stretch, Carboxylic acid
3357.995	N-H stretch, Aliphatic primary amine
3438.906	N-H stretch, Primary amine
3558.829	O-H stretch, Alcohol
3690.117	O-H stretch, Alcohol

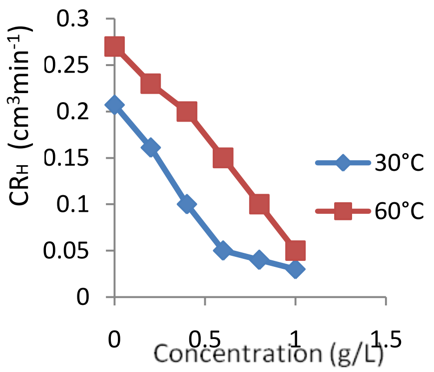

Figure 3: Effect of concentration on the rate of hydrogen evolution (CH_R)

The effect of concentration of extract on the rate of hydrogen evolution (which can be correlated to corrosion rate (Obot *et al.*, 2011) in HCl solution at 30 and 60°C from the gasometric method is presented in Figure 3.

The rate of hydrogen evolution at 0.0 g/L is higher compared to the values obtained at various concentrations of the extract. This implies that the flower extract of *Cucurbita pepo* mitigated the corrosion of mild steel in the acidic medium. The rate of hydrogen evolution was also observed to decrease with increase in the concentration of the flower extract. The trends obtained from the gasometric method are in complete agreement with the trends from the weight loss method.

Effect of concentration on the inhibition efficiency of the extract

Figures 4 and 5 show the effect of concentration on the inhibition efficiency of the plant extract obtained from the two methods of corrosion measurement. The inhibition efficiency of the extract was observed to increase with increase in concentration at all temperatures. Maximum inhibition efficiencies were obtained at concentration of 1.0 g/L. A comparison of the inhibition efficiency of the extract at 30 and 60°C showed that inhibition efficiency decreased with increase in temperature at all concentrations probably due to the increased rate of dissolution of the metal in the acidic medium (Fadare *et al.*, 2016). This signifies physical adsorption (Obot *et al.*, 2011). This is in agreement with findings by Chahul *et al.* (2019).

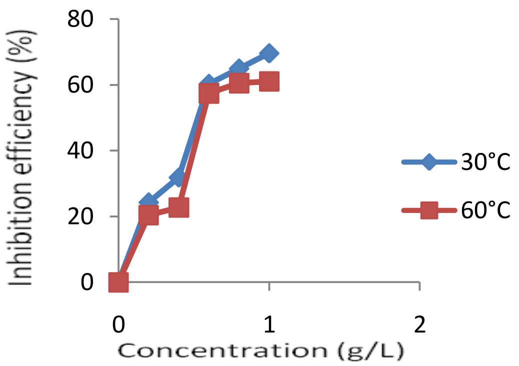

Figure 4: Effect of concentration on the inhibition efficiency of the extract obtained by gravimetric method

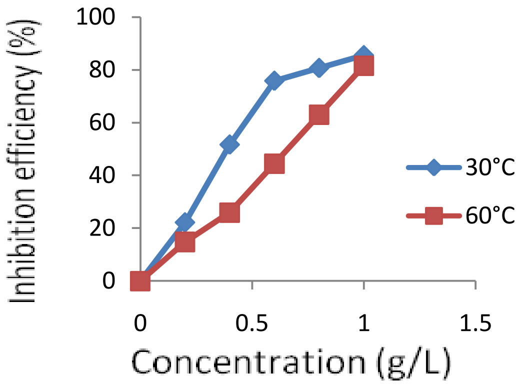

Figure 5: Effect of concentration on the inhibition efficiency of the extract obtained by gasometric method

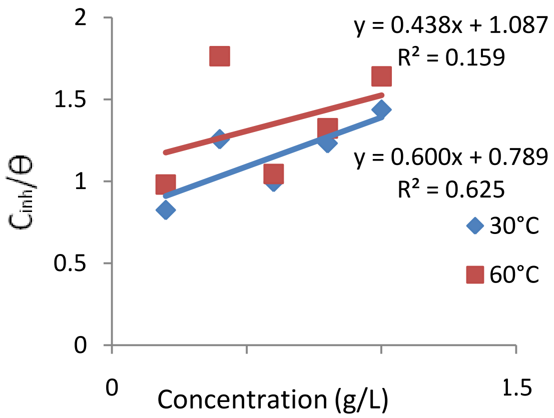

Figure 6: Langmuir adsorption isotherm plots for the adsorption of the extract on the metal surface in HCl solution at 30 and 60°C

Table 4: Langmuir adsorption isotherm parameters for the adsorption of the extract on the metal surface in the acid medium

Parameter	Temp (K)	
	303	333
Slope	0.6	0.44
R^2	0.63	0.16
K_{ads}	1.27	0.92
ΔG^o_{ads}	-10.72	-10.89

Adsorption considerations

Langmuir and Temkin adsorption isotherm models were used to investigate the adsorption characteristics of the extract on the mild steel surface. Langmuir isotherm assumes uniform energies of adsorption onto the metal surface and no transmigration of adsorbate in the plane of the surface (Dada *et al.*, 2012). The linear form of the Langmuir adsorption isotherm is represented by Equation 5 (Iorhuna and Ayuba, 2023).

$$\frac{C_{inh}}{\theta} = \frac{1}{K_{ads}} + C_{inh} \qquad 5$$

where C_{inh} is the inhibitor concentration, ϴ is the surface coverage and K_{ads} is the adsorption equilibrium constant. The plot of $\frac{C_{inh}}{\theta}$ versus C_{inh} is shown in Figure 6. Linear plots were obtained with coefficient of correlation (R^2) not close to unity.

This is an indication that the experimental data did not fit the Langmuir adsorption isotherm model (Paul and Koley, 2016). This does not agree with the result obtained by Chahul *et al.* (2019). The values of Langmuir adsorption isotherm parameters obtained from the plots are presented in Table 4.

The adsorption equilibrium constant (K_{ads}) decreased with increase in temperature. Large values of K_{ads} signifies better inhibition efficiency (Okafor and Ebenso, 2007), therefore the extract was more efficient at 30°C. The free energy of adsorption (ΔG^o_{ads}) was computed using Equation 6 and the result is presented in Table 4. The values of ΔG^o_{ads} were all negative which implies that the adsorption process is spontaneous (Ali *et al.*, 2021). Also, the calculated values of ΔG^o_{ads} were not up to -40 KJ/mol which is indicative of physical adsorption (Chahul *et al.*, 2019).

$$\Delta G^o_{ads} = -2.303RTLog(55.5K_{ads}) \qquad 6$$

Temkin adsorption isotherm model assumes that the heat of adsorption of all the molecules in the layer decreases linearly with coverage due to adsorbent-adsorbate interactions and the adsorption is characterized by a uniform distribution of the bonding energies, up to some maximum binding energy (Temkin and Pyzhev, 1940; Oladoja *et al.*, 2008 cited in Fadare *et al.*, 2016). The linear form of the Temkin adsorption isotherm is represented by the expression in Equation 7 (Fadare *et al.*, 2016).

$$\Theta = BInA + BInC \qquad 7$$

where A(L/g) is the equilibrium binding constant, C is the extract concentration and B is related to the heat of adsorption. The plot of ϴ against In C is shown in Figure 7. Liner plots were obtained with very good coefficient of correlation (R^2) which implies that the experimental data fitted into the Temkin adsorption isotherm model.

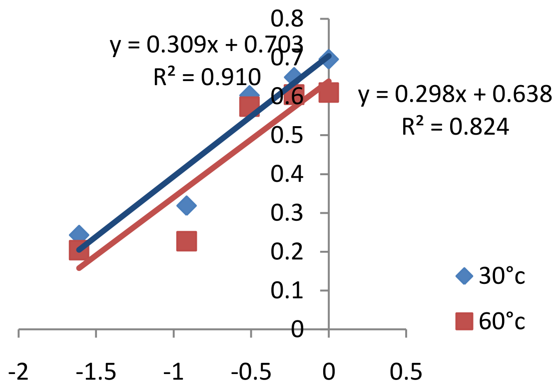

Figure 7: Temkin adsorption isotherm plots for the adsorption of the extract on the metal surface in HCl solution at 30 and 60°C

Table 5: Temkin adsorption isotherm parameters for the adsorption of the extract on the metal surface in the acid medium

Parameter	Temp (K)	
	303	333
B	0.31	0.30
R^2	0.91	0.82
A	9.73	8.51
ΔG^o_{ads}	-15.85	-17.05

The values of B and A were determined from the slope and intercept of the plots (Fadare *et al*., 2016). Values of the Temkin adsorption isotherm parameters are presented in Table 5.

The value of the equilibrium binding constant (A) at 30°C is higher compared to the value at 60°C. This implies that the extract performed better at 30°C. The ΔG^o_{ads} values obtained from Equation 5 were all negative and not up to -40 KJ/mol. This implies that the adsorption of the extract on the metal surface is a spontaneous process and suggests physical adsorption mechanism (Iorhuna and Ayuba, 2023).

Thermodynamic studies

The Arrhenius equation (Equation 8) is used to determine the effect of temperature on the corrosion rate of mild steel in the acidic medium (Iorhuna and Ayuba, 2023).

$$\text{LogCR} = \text{LogA} - \frac{E_A}{2.303RT} \qquad 8$$

where CR is the corrosion rate of mild steel, A is the Arrhenius constant, E_a is the apparent activation energy, R is the universal gas constant and T is the temperature in Kelvin. The Arrhenius plot for the corrosion of mild steel in the acidic solution with the extract is presented in Figure 8.

The apparent activation energy (E_a) at each concentration was obtained from the slope of the plot (i.e slope = $-\frac{E_a}{2.303R}$) (Iorhuna and Ayuba, 2023). These values (E_a) are presented in Table 6.

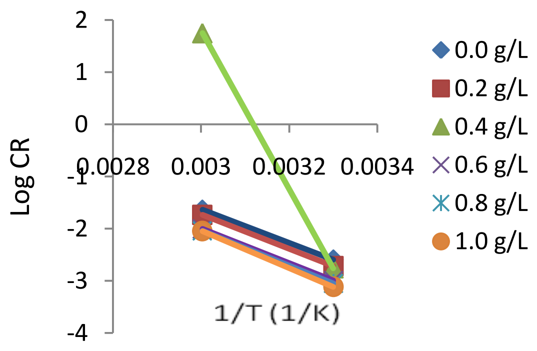

Figure 8: Arrhenius plots for the corrosion of mild steel in 0.5 M HCl solution with different extract concentrations

Table 6: Activation energy (E_a) values for the corrosion of mild steel in the acidic solution

Concentration (g/L)	E_a (KJ/mol)
0.0	61.67
0.2	63.26
0.4	290.86
0.6	63.61
0.8	65.06
1.0	68.74

The apparent activation energy at various concentrations of the extract is higher compared to the value obtained in the blank (0.0 g/L) solution. Similar result was also reported by Chahul *et al*. (2019). The increase in activation energy in the presence of the extract signifies physical adsorption (Iorhuna and Ayuba, 2023).

CONCLUSION

The flower of *Cucurbita pepo* could serve as a green corrosion inhibitor for metals in acidic media. The inhibition efficiency of the plant part is affected by temperature.

REFERENCES

Abdulrahman, A. S., Ganiyu, K. A., Kobe, I. C. and Awe, I. C. (2015). The corrosion inhibition of mild steel in sulphuric acid solution by adsorption of *African perquetina* leaves extract. *Int. J. Innov. Res. Sci., Eng. & Tech.*, 4(4), 1809-1821. doi: 10.15680/IJIRSET.2015.0404002

Ali, A. E., Badr, G. E. and Fouda, A. S. (2021). *Citrus sinensis* extract as a green corrosion inhibitor for the corrosion of carbon steel in sulphuric acid solution. *Biointerf. Res. Appl. Chem.*, 11(6), 14007-14020. https://doi.org/10.33263/BRAIAC116.14007140 20

Al–Otaibi, M. S., Al-mayouf, A. M., Khan, M., Mousa A. A., Al-mazroa, S. A. and Alkhathlan, H. Z. (2012). Corrosion inhibitory action of some plant extracts on the corrosion of mild steel in acidic media. *Arab. J. Chem.*, 7(3), 340-346. http://dx.doi.org/10.1016/j.arabjc.2012.01.015

Ayuba, A. M. and Abubakar, A. (2021). Inhibiting aluminium acid corrosion using leaves extract of *Guiera senegalensis. J. Fund. & Appl. Sci.*, 13(2), 634-656. http://dx.doi.org/10.4314jfas.v13i2.1

Bucaretchi, F., Dragosavac, S. and Vieira, R. J. (2003). Acute exposure of imidazoline derivates in children. *J. de Pediat.*, 79(6), 519 -524.

Chahul, H. F., Danat, B. T. and Maji, E. (2019). Corrosion inhibition of ethanol extract leaves of *Cucurbita pepo* (Pumpkin) on mild steel in acidic media. *Chem. Search J.*. 10(1), 46-53.

Dada, A. O., Olalekan, A. P. Olatunya, A. M. and Dada, O. (2012). Langmuir, Freundlich, Temkin and Dubinin – Radushkevich isotherms studies of equilibrium sorption of Zn^{2+} unto phosphoric acid modified rice husk. *IOSR J. Appl. Chem.*, 3(1), 38-45.

Elachi, E. E., Justine, A., Paul, M. Yusuf, K. D. and Madugu, A. B. (2022). Corrosion inhibition potentials of Roselle (*Hibiscus sabdariffa*) in tetraoxosulphate (VI) acid solution. *Int. J. Eng. & Appl. Phys*., 2(3), 524-534.

Giwa, A. A. Adetunji, A. T. and Wewers, F. (2020). Assessment of Negro pepper (*Xylopia aethiopica*) fruit extracts as corrosion inhibitors for mild steel. *J. Mat. & Environ. Sci.*, 11(7), 1100-1111.

Hassan, H. K., Khadom, A. A and Kurshed, N. H. (2016). *Citrus aurantium* leaves extract as a sustainable corrosion inhibitor of mild steel in sulfuric acid. *Sou. Afr. J. Chem. Eng.*, 22(2), 1-5. http://dx.doi.org/10.1016/j.sajce.2016.07.002

Hussain, G. (2023). Soxhlet extraction, principle, working and usage. Retrieved from https://www.researchgate.net/publication/372658021. Retrieved on 2nd March, 2024.

Ibisi, N. E. and Ugochukwu, C. V. (2015). *Dennettia tripetala* extract as green corrosion inhibitor of mild steel in hydrochloric acid. *Global J. Environ. Sci. & Tech*., 2(6), 349-354.

Iorhuna, F. and Ayuba, A. M. (2023). Mild steel corrosion inhibition in acidic media using *Sarcocephalus latifolius* leaves extract. *J. Fund. Appl. Sci.*, 15(2), 176-193. http://dx.doi.org/10.4314/jfas.1277

Loto, C. A., Loto R. T and Joseph, O. O. (2017). Effect of Benzamide on the corrosion inhibition of mild steel in sulphuric acid. *Sou. Afri. J. Chem.*, 70, 38-43. http://dx.doi.org/10.17169/0379-4350/2017/v70a6

Lqaz, H., Masroor, S., Chafia, M., Ali, I. H., Alghamdi, M. M., Chaouiki, A. and Chungii, I. (2020). Evaluation of 2-mercaptobenzimidazole derivatives as corrosion inhibitors for mild steel in hydrochloric acid. *Metals*, 10, 357. https://doi.org/10.3390/met10030357

Nandiyanto, A. B. D., Oktiani, R and Ragadhita, R. (2019). How to read and interpret FTIR spectroscope of organic material. *Indonesian J. Sci. & Tech*., 4(1), 97-118. http://dx.doi.org/10.17509/ijost.v4i1.15806

Obot, I. B., Umoren, S. A. and Obi-Egbedi, N. O. (2011). Corrosion inhibition and adsorption behavior for aluminuim by extract of *Aningeria robusta* in HCl solution: synergistic effect of iodide ions. *J. Mater. Environ. Sci.*, 2(1), 60-71.

Ogunleye, O. O., Arunkoola, A. O., Eletta, O. A., Agbede, O. O., Osho, Y. A., Movakinyo, A. F. and Hamed, J. O. (2020). Green corrosion inhibition and adsorption characteristics of *Luffa cylindrica* leaf extract on mild steel in hydrochloric acid environment. *Heliyon*, 6, 1-12. https://doi.org/10.1016/j.heliyon.2020.e03205

Okafor, P. C. and Ebenso, E. E. (2007). Inhibitive action of *Carica papaya* extracts on the corrosion of mild steel in acidic media and their adsorption characteristics. *Pigm. Res. Tech.*, 36(3), 134-140. https://doi.org/10.1108/03699420710748992

Paul, S. and Koley, I. (2016). Corrosion inhibition of carbon steel in acidic environment by Papaya seed as green inhibitor. *J. Bio. & Tribo corr.*, 2(6), 1-9. doi: 10.1007/s40725-016-0035-2

Stuart, B. (2004). Infrared spectroscopy: fundamentals and applications. USA, John Wiley and Sons.

Umoren, S. A. and Eduok, U. M. (2016). Application of carbohydrates in different media: review. *Carb. Poly.*, 140, 314-341.

Uwah, I. E. Okafor, P. C. and Ebiekpe, V. E. (2013). Inhibitive action of ethanol extracts from *Nauclea latifolia* on the corrosion of mild steel in H_2SO_4 solutions and their adsorption characteristics. *Arab. J. Chem.*, 6, 285-293. doi: 10.1016/j.arabjc.2010.10.008